

Battery Reliability of fast Electric Vehicle Charging Systems

Karunarathna, Jayani; Madawala, Udaya; Baguley, Craig; Blaabjerg, Frede; Sandelic, Monika

Published in:

Proceedings of the 2021 IEEE Southern Power Electronics Conference (SPEC)

DOI (link to publication from Publisher):

[10.1109/SPEC52827.2021.9709461](https://doi.org/10.1109/SPEC52827.2021.9709461)

Publication date:

2021

Document Version

Accepted author manuscript, peer reviewed version

[Link to publication from Aalborg University](#)

Citation for published version (APA):

Karunarathna, J., Madawala, U., Baguley, C., Blaabjerg, F., & Sandelic, M. (2021). Battery Reliability of fast Electric Vehicle Charging Systems. In *Proceedings of the 2021 IEEE Southern Power Electronics Conference (SPEC)* (pp. 1-6). Article 9709461 IEEE Press. <https://doi.org/10.1109/SPEC52827.2021.9709461>

General rights

Copyright and moral rights for the publications made accessible in the public portal are retained by the authors and/or other copyright owners and it is a condition of accessing publications that users recognise and abide by the legal requirements associated with these rights.

- Users may download and print one copy of any publication from the public portal for the purpose of private study or research.
- You may not further distribute the material or use it for any profit-making activity or commercial gain
- You may freely distribute the URL identifying the publication in the public portal -

Take down policy

If you believe that this document breaches copyright please contact us at vbn@aub.aau.dk providing details, and we will remove access to the work immediately and investigate your claim.

Battery Reliability of Fast Electric Vehicle Charging Systems

Jayani Karunarathna¹, Udaya Madawala¹, Craig Baguley², Frede Blaabjerg³, and Monika Sandelic³

¹*Department of Electrical and Computer Engineering, The University of Auckland, Auckland, New Zealand*
dkar412@aucklanduni.ac.nz, u.madawala@auckland.ac.nz

²*Department of Engineering, Computer and Mathematical Sciences, Auckland University of Technology, Auckland, New Zealand*
craig.baguley@aut.ac.nz

³*Department of Energy, Aalborg University, 9220 Aalborg, Denmark*
fbl@energy.aau.dk, mon@energy.aau.dk

Abstract—Fast electric vehicle charging systems (FEVCSs) are becoming popular, but to assure long-term operation, further research on battery lifetime is necessary. This is because FEVCSs use high charging currents, and consequently subject Li-Ion batteries to high levels of average state of charge (SOC) and temperatures within a short period of time. Thus, degradation mechanisms, such as Lithium plating and electrolyte breakdown, are inevitable in Li-Ion batteries, leading to reduced battery capacity and lifetime. Therefore to investigate the battery reliability of FEVCSs, this paper proposes a two-stage modeling approach. Using the proposed model, the impact of SOC and temperature on the reliability of the battery as well as the reliability of a Li-Ion battery under typical fast EV charging conditions are investigated, and results are presented to show how the battery reliability deteriorates under fast charging conditions.

Keywords—Reliability, lifetime, mission profile, battery, fast electric vehicle charging systems

I. INTRODUCTION

At present, the ever-increasing Carbon emissions in the environment is a significant concern. Conventional vehicles that depend solely on internal combustion engines (ICEs) are the major contributor to high CO₂ emissions [1]. Therefore, eco-friendly electric vehicles (EVs) are becoming an attractive alternative to ICE vehicles. However, shorter range per charge and longer recharging time are the major concerns of EV users that need addressing to increase the EV uptake. Thus, development of batteries with high energy density and fast (rapid) charging capability has become a research focus in EV charging systems. Amongst various battery technologies, Li-Ion batteries have been predominately used in EV applications due to their high efficiency, fast response time, scalability, and low self-discharge rate [2, 3]. However, the development of low cost, compact and reliable batteries for fast EV charging systems (FEVCSs) has still been a challenge.

The rate of charging or discharging of a battery cell is limited by the rate at which the active chemicals in the cells can be transformed. This is because there are different reaction gradients between the ions close to the electrodes, those further away and also within the electrodes themselves of a battery cell. Thus, forcing high currents through the battery results in an incomplete transformation of active chemicals and also causes unwanted, irreversible chemical reactions [4]. The incomplete transformations can result in the deposition of surplus ions on the anode in the form of Lithium metal. This is known as Lithium plating, which leads to irreversible loss of battery capacity. The unwanted chemical reactions consume some of the active chemicals, causing the battery to lose capacity and therefore to age prematurely. This may be

accompanied by changes in the structure of electrode crystals such as crystal growth or cracking, which have a negative impact on the internal impedance of the battery cell. At the same time, maintaining high currents and voltages during fast charging may result in electrolyte breakdown, resulting in further loss in capacity. Therefore, with each charge/discharge cycle, the accumulated irreversible reduction in battery capacity is expected to increase and, eventually, the reduction in capacity will result in the cell being unable to store the amount of energy that is required. In other words, it reaches the end of its useful life. Since the loss of capacity is caused by the high current operation, it can be expected that higher is the current the shorter is the cycle life of the cell [5]. Accordingly, the batteries in FEVCSs are expected to degrade/wear-out at much faster rate and need to be replaced a few times within the lifespan of the charging system. Therefore to avoid the unnecessary accelerated battery degradation, the battery reliability must be analysed and taken into account first when implementing the charging algorithms for FEVCSs.

According to the literature, battery reliability analysis depends on the application-specific operating conditions [6]. In [7] and [8], battery lifetime analysis models have been developed for grid-support applications. Another research on lifetime modeling of batteries in photovoltaic application have been carried out in [6] and [9]. In relation to EVs, different studies have investigated the lifetime of batteries, and various empirical models have been built based on experimental results. The battery capacity fade during the discharging process has been discussed in [10], and a model to analyse the battery degradation has been developed in [11]. Studying the battery ageing according to different usage patterns has been considered in [12]. In these methods, intensive experimental work is performed on the battery in the laboratory and the results are fit to mathematical functions to develop a model. However, these studies generally focus on the battery itself in specific laboratory conditions, and require significant effort and time. The operating fluctuations originated from traffic flow dynamics, varying mechanical forces and road conditions on the battery performance have been studied in [13]. Other factors that affect the EV battery in vehicle-to-grid (V2G) applications and its aging have been explored in [14–16]. However, more research in relation to EV applications is still needed as development of comprehensive analytical battery lifetime models and the extension of battery lifetime models in a probabilistic manner to perform reliability analysis are yet to be carried-out. Moreover, since fast EV charging is becoming popular, reliability analysis of batteries in FEVCSs is important to ensure robust operation under fast charging conditions.

Therefore this paper proposes a comprehensive reliability analysis model for Li-Ion batteries in FEVCSs. In this study, a two-stage analytical modeling approach based on electro-thermal simulation is used to determine the battery lifetime and reliability. The rest of the paper is structured as follows. The paper discusses a typical FEVCS configuration in Section II. The reliability analysis model with a two-stage modeling approach is explained in Section III. In Section IV, a case study based on a three-phase 80 kW FEVCS is presented to demonstrate how the battery reliability deteriorates under fast charging conditions. Finally, conclusions are given in Section V.

II. FAST EV CHARGING

According to the society of automotive engineers (SAE) J1772 standard, EV charging is classified into four levels. AC level 1 is the slowest way of charging an EV. A domestic 120 V outlet and less than 2 kW of charging power are used in this level. AC level 2 charges the EV 10 times faster than the AC level 1 charging. Typically, AC level 2 charging uses a 5 kW to 19 kW charging power, which is the most commonly used level for daily EV charging. DC level 1 and level 2 charging are the fastest ways to charge an EV. DC level 1 uses charging power up to 80 kW, while DC level 2 uses charging power up to 400 kW. Usually, AC chargers are on-board chargers. These chargers convert AC power into DC using the power electronic converters placed inside the vehicle. Unlike AC chargers, DC fast chargers use DC to charge the EV. Because of the high charging power levels in DC fast charging, it is difficult to carry the required components on-board due to size constraints. Therefore, DC fast chargers are typically off-board chargers, and the conversion of power from AC to DC usually takes place at the charging station [17]. However, DC fast chargers cost tens of thousands of dollars, and working with a high level of power, user safety, efficient power conversion and reliability of the charging system are critical in DC fast chargers.

In order to analyse the reliability of a Li-Ion battery, charged by a typical three-phase FEVCS shown in Fig. 1, is

considered. This charging system consists of two interconnected power electronic converters, a three phase AC/DC converter and a DC/DC converter. The three-phase AC/DC converter, which is fed by a 400 V AC supply, draws a sinusoidal current and maintains the DC link voltage at 600 V. The DC/DC converter is a phase-shift controlled dual active bridge, with input and output DC voltages being 600 V and 384 V, respectively, and operated at 20 kHz. The DC/DC converter regulates the power flow required to charge the battery while providing galvanic isolation.

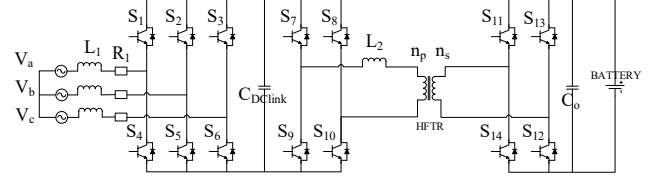


Fig. 1. A typical three-phase fast EV charging system.

III. RELIABILITY ANALYSIS MODEL

Fig. 2 presents the proposed battery reliability analysis model, comprising a two-stage modeling approach which is given below.

Stage 1: Translation of mission profile into stress profiles

- Mission profile interpretation
- Stress profile interpretation

Stage 2: Reliability estimation

- Rainflow cycle counting
- Lifetime modeling
- Lifetime distribution
- Reliability evaluation

The steps in the two stages of the reliability analysis model will be explained in details in the following sections.

A. Mission Profile Interpretation (Stage 1)

The battery lifetime can be mainly influenced by the operating conditions of the system. Thus, in order to estimate

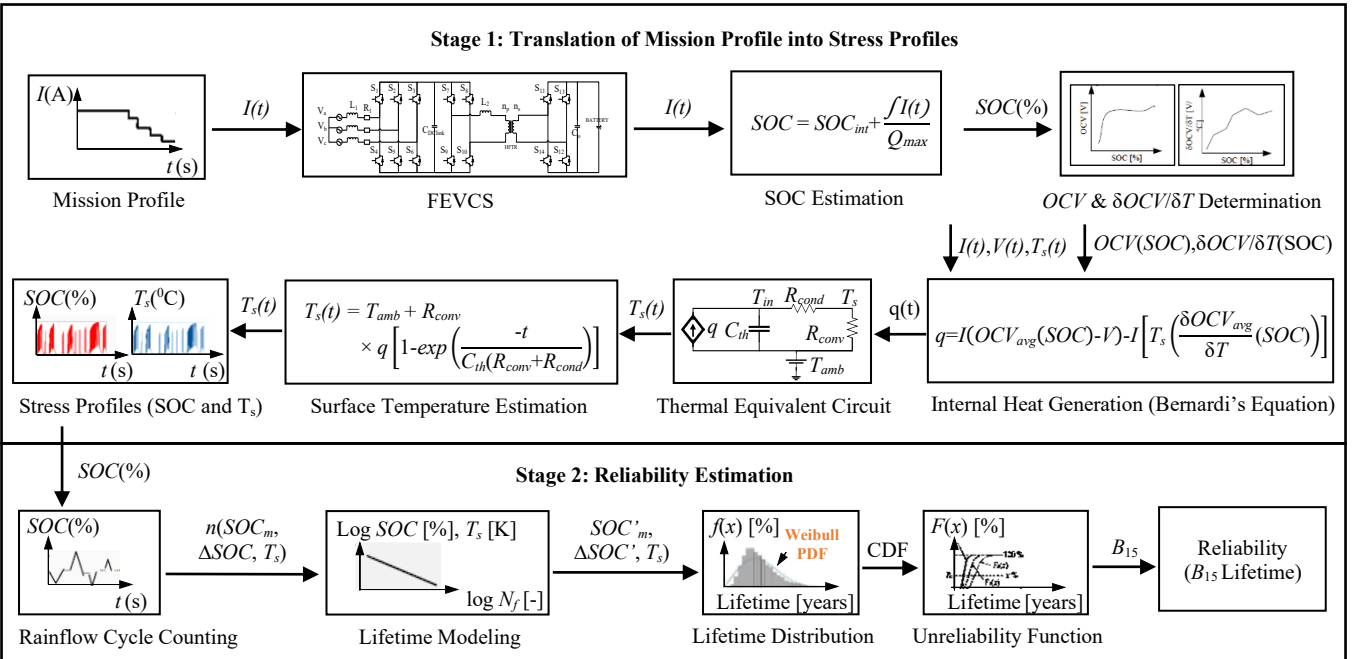


Fig. 2. Reliability analysis model.

the battery reliability, the operating conditions throughout the charging process must be known [18]. In this respect, a mission profile representing the operating conditions of the battery is needed. The charging profile of the FEVCS is directly related to the operating conditions of the fast EV charger. Therefore, the charging profile is considered as the mission profile. Amongst different EV charging strategies, multistage constant current (MSCC) charging is the most preferred method for fast charging. Hence, the MSCC charging profile is used in this study. The method described in [19] is considered to implement the MSCC charging profile with optimal current levels, which results in minimum charging time. There are five current level stages in the MSCC charging profile. The current levels at different stages are used for the reference currents in the current controller of the DC/DC converter. The battery is charged with the current levels in each stage until the battery voltage reaches a predefined maximum permissible value.

B. Stress Profile Interpretation (Stage 1)

The principal deterioration mechanism in batteries is the electrolyte loss, which results in a reduction in capacity, for which the battery state of charge (SOC) and surface temperature (T_s) being the most relevant stress variables. Therefore, the battery SOC and T_s need to be derived from the mission profile to represent the real operating conditions. Hence to obtain the SOC, the current levels in the charging profile are used as the input to Stage 1 of the model, and SOC is obtained as:

$$SOC = SOC_{int} + \frac{\int I(t)}{Q_{max}} \quad (1)$$

where SOC_{int} , $I(t)$ and Q_{max} are initial SOC, charging current and maximum capacity of the battery, respectively. T_s can be determined using internal heat generation (q) and thermal equivalent circuit of the battery cell. The q can be calculated using Bernardi's equation as:

$$q = I (OCV_{avg}(SOC) - V) - I \left[T_s \left(\frac{\delta OCV_{avg}}{\delta T}(SOC) \right) \right] \quad (2)$$

where V is the battery terminal voltage, and $OCV_{avg}(SOC)$ and $\delta OCV_{avg}/\delta T(SOC)$ are open circuit voltage and entropic heat coefficient of the battery cell at a certain SOC, respectively. The look-up table (LUT) approach in the PLECS simulator is used to obtain the OCV_{avg} and $\delta OCV_{avg}/\delta T$. In this regard, under a particular set of operating conditions, the OCV_{avg} and $\delta OCV_{avg}/\delta T$ are obtained in advance and the OCV_{avg} and $\delta OCV_{avg}/\delta T$ for the required operating conditions are then interpolated using the LUT. After calculating the q , battery T_s can be obtained as:

$$T_s(t) = T_{amb} + R_{conv} \times q \left[1 - \exp \left(\frac{-t}{C_{th}(R_{conv} + R_{cond})} \right) \right] \quad (3)$$

where T_{amb} , R_{conv} , R_{cond} , C_{th} and t are ambient temperature, convection resistance, conduction resistance, thermal capacitance and operation time of the battery, respectively. The parameters R_{conv} , R_{cond} and C_{th} of the battery are calculated according to the method described in [20]. Thus, the battery SOC and T_s for a certain mission profile can be obtained.

C. Rainflow Cycle Counting (Stage 2)

A cycle counting method must be used to extract the cycling distribution of the SOC stress profile, which is needed as an input parameter for the battery lifetime model. Hence,

the Rainflow cycle counting method, which is a widely used approach for extracting cycle information, is used to extract the cycles in the SOC profile [21]. Usually, the extracted cycle data are stored in a matrix form referred to as a Rainflow matrix. Thus, the required parameters such as the mean SOC (SOC_m), SOC cycle amplitude (ΔSOC), and the number of cycles (n) can be obtained from the Rainflow matrix and used directly in the battery lifetime model.

D. Lifetime Modeling (Stage 2)

The lifetime model of the battery provides the information of the battery capacity fade, which occurs due to ageing. Li-Ion batteries are ageing during both storage and operation. Ageing during storage is referred to as calendar ageing and ageing during operation is referred to as cycling ageing. The calendar ageing of Li-Ion batteries is mainly enhanced by high SOC levels and high temperatures, which are causing both power capability decrease and capacity fade [22, 23]. The cycling ageing of Li-Ion batteries is mainly influenced by the high SOC levels, the SOC cycle depth, the charging/discharging C-rate and temperature, which are also causing both power capability decrease and capacity fade [24, 25]. Expression for capacity fade is defined as [26]:

$$C_{ca} = 1.9775 \times 10^{-11} \times e^{0.07511 \times T_s} \times 1.639 \times 10^{0.00738 \times SOC_m \times t^{0.8}} \quad (4)$$

$$C_{cy} = 2.6418 \times e^{-0.01943 \times SOC_m \times (0.004 \times e^{0.01705 \times T_s})} \times (0.0123 \times \Delta SOC^{0.7162}) \times n^{0.5} \quad (5)$$

$$C_f = C_{ca} + C_{cy} \quad (6)$$

where C_{ca} , C_{cy} , C_f and t are the capacity fade due to calendar aging, capacity fade due to cycling, total capacity fade of the battery and operation time, respectively. The input parameters, SOC cycle information, SOC_m , ΔSOC , and n , can be determined from the Rainflow cycle counting method described above. The T_s can be obtained according to the method explained in Section III. B. The battery lifetime is usually described in terms of life consumption (LC). According to Palmgren Miner's rule [27], the LC of the battery during the operation can be calculated as:

$$LC = \sum_i C_{fi} \quad (7)$$

where C_{fi} is the capacity fade for a particular SOC_m and ΔSOC . When the LC accumulates to 0.7, which corresponds to a 30% capacity fade, the battery is considered to be at the end of its life.

E. Lifetime Distribution (Stage 2)

The battery lifetime predictions obtained from (7) can be considered as an ideal case in which all the components have the same failure rate. In reality, there are uncertainties in the lifetime prediction due to manufacturing variations, differences in the lifetime model parameters and stress changes. In order to consider these uncertainties, it is required to perform the Monte Carlo analysis [28] by introducing lifetime model parameter variations and determining the lifetime with a large sample size. With a significant sample size, the results will then converge to the required value. Thus, the lifetime predictions can be presented in terms of a statistical value rather than a fixed value by taking into account the system parameter variations. In this approach, the

parameters in the lifetime model described in (4) and (5) must be modeled by a specific distribution function introducing a certain parameter variation range. Thus, by performing the Monte Carlo simulation, the lifetime distribution $f(x)$ for the battery can be obtained from the lifetime data of the selected number of samples.

F. Reliability Evaluation (Stage 2)

The lifetime distribution $f(x)$ of the battery follows a Weibull distribution [20], with the probability density function (PDF) given as [30]:

$$f(x) = \frac{\beta}{\eta^\beta} x^{\beta-1} \exp \left[-\left(\frac{x}{\eta} \right)^\beta \right] \quad (8)$$

where β is the shape parameter and η is the scale parameter. β usually indicates the failure mode, while η represents the time when 63.2% of the population has failed [30]. Using the PDF of the Weibull distribution, it is possible to obtain the cumulative distribution function (CDF) by integration over the operation period. The CDF is referred to as an unreliability function $F(x)$ which indicates the development of failure population over time. Consequently, using the unreliability function, the B_{15} lifetime of the battery, which is used as a reliability metric, can be obtained. The quantity, B_{15} lifetime represents the time taken for 15% of the population to fail [30]. Thus, by considering the unreliability function, the reliability or the B_{15} lifetime of the battery can be determined.

IV. CASE STUDY

A. Mission Profile of the Case Study

In order to investigate the battery reliability, a case study of a Li-Ion battery in a typical three-phase 80 kW FEVCS, shown in Fig. 1, was considered. The battery SOC and T_s were determined by charging the battery for 20 minutes period with a MSCC charging profile, as illustrated in Fig. 3. The battery was charged with five stages of current levels, and currents in each stage were applied to the battery until the battery voltage reached a predefined maximum permissible value.

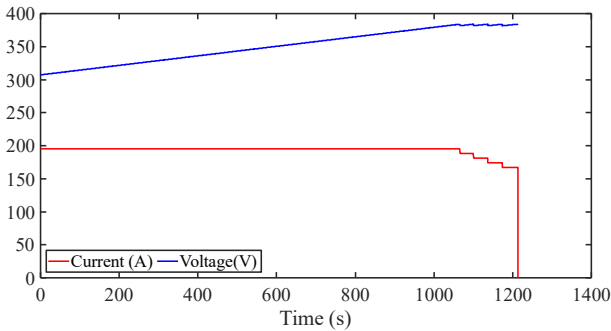


Fig. 3. Fast EV charging profile.

B. Battery SOC and T_s Profiles

Using the approach of mission profile translation outlined in Section III. B, the battery SOC and T_s were obtained and depicted in Fig. 4 and Fig. 5, respectively. In order to ensure safe and long-term operation, the battery SOC is usually limited to a certain range in FEVCSs. Hence as shown in Fig. 4, the battery was charged from 20% to 80% SOC within 20 minutes by feeding the MSCC charging profile. According to Fig. 5, it can be observed that the T_s of the battery reaches its highest value of 46.7 °C, while its mean value is 40 °C when the battery was charged under air-cooling conditions.

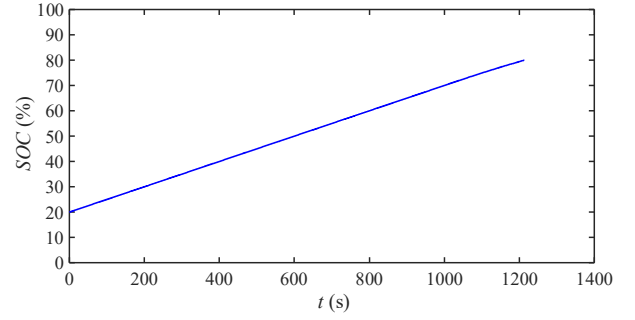


Fig. 4. Battery SOC profile.

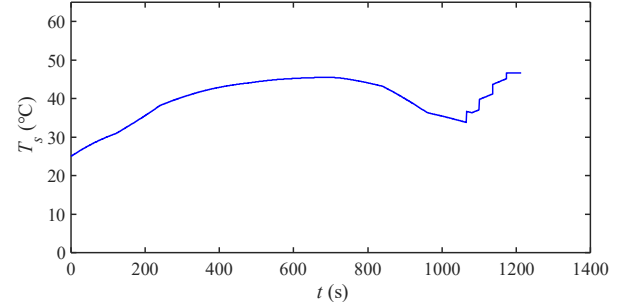


Fig. 5. Battery T_s profile.

C. Translated SOC Profile with Cycle Counting

As described in Stage 2, the Rainflow cycle counting was performed to organize the SOC profile in a manner that was appropriate for the lifetime model. By doing so, the mean value, cycle amplitude and the number of cycles of the SOC profile were obtained. The resultant Rainflow matrix histogram for the battery SOC is shown in Fig. 6. The SOC cycles have a SOC_m value of 50.32% during the charging and 49.9% during the discharging, with a ΔSOC of about 30%.

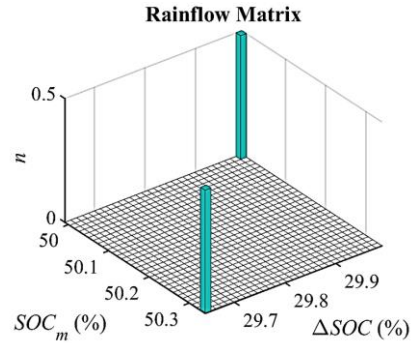


Fig. 6. Rainflow matrix of the battery SOC.

D. Lifetime and Reliability Evaluation

By applying the Rainflow cycle counting results and the battery T_s into (7), the corresponding LC of the battery was calculated. The resultant LC of the battery is 0.1223/year. This implies that the battery is expected to reach its end of useful life that is 70% of battery capacity, after 6 years of operation.

Furthermore, by introducing parameter variances into the lifetime model, the Monte Carlo simulation was employed to simulate the lifetime with a large number of samples. In this regard, each parameter in the lifetime model described in (4) and (5) was modeled by a normal distribution with a 5% parameter variation. Thus, a set of lifetime data were obtained with a population of 10000 samples and represented by a

lifetime distribution. The obtained lifetime distribution along with the corresponding Weibull distribution is depicted in Fig. 7. According to the lifetime distribution of the battery, it can be observed that the lifetime of most of the samples lies near to 6 years, which is equal to the lifetime of the battery calculated with one sample.

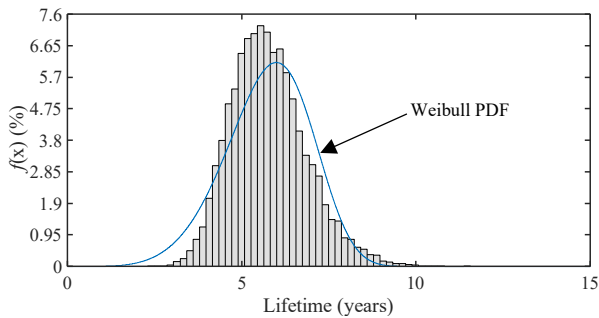


Fig. 7. $f(x)$ and the corresponding Weibull PDF of the battery.

By integrating the obtained lifetime distribution over the operation time, the unreliability function for the battery was obtained and presented in Fig. 8. According to the unreliability function, the reliability of the battery, which is represented by the B_{15} lifetime, under fast charging conditions is 4.5 years. This implies that 15% of the population of batteries under fast charging conditions is expected to fail after 4.5 years. According to the manufacture data, batteries in slow electric vehicle charging systems (SEVCSs) last for at least 8 years. Thus, results indicate that batteries in FEVCSs are expected to fail around 3.5 years earlier than the batteries in SEVCSs. Furthermore, it is important to note that the reliability analysis presented here can be further extended to improve the battery reliability by introducing rest periods during the charging and introducing advanced cooling methods.

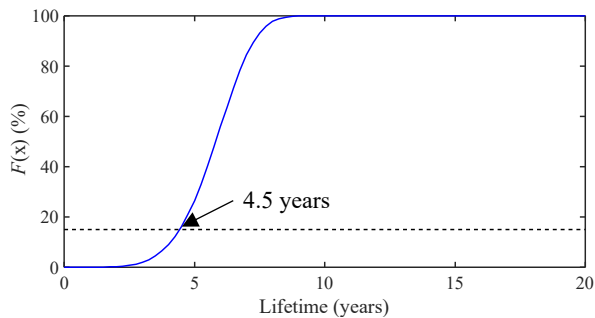


Fig. 8. $F(x)$ of the battery.

V. CONCLUSION

In this paper, a two-stage modeling approach has been presented to investigate the reliability of batteries in FEVCSs. Within each stage, systematic mathematical and simulation models have been developed to analyse the impact of SOC and temperature on the battery reliability. Using the proposed modelling approach, the reliability of a Li-Ion battery has been investigated under typical fast EV charging conditions, and results have been presented showing how battery reliability deteriorates under fast charging conditions. The proposed reliability analysis model is expected to be a valuable tool when designing reliable FEVCSs.

REFERENCES

- [1] I. E. Agency and I. U. of Railways, "Railway Handbook 2015," 2015.
- [2] B. Scrosati, J. Garche, "Lithium batteries: status, prospects and future," *Journal of Power Sources*, vol. 195, no. 9, pp. 2419-2430, May 2010.
- [3] P. N. Oyama, T. Tatsuma, T. Sato and T. Sotomura, "Dimercaptan-polyaniline composite electrodes for lithium batteries with high energy density," *Nature*, vol 373, pp. 598-600, 1995.
- [4] B. Lawson, Battery life (and death), *The Electropaedia*. Accessed on: Nov. 2, 2019. [Online]. Available: <http://www.mpoweruk.com/life.htm>.
- [5] S. S. Choi and H. S. Lim, "Factors that affect cycle-life and possible degradation mechanisms of a li-ion cell based on LiCoO_2 ," *Journal of Power Sources*, vol. 111, no. 1, pp. 130-136, 18 Sep 2002.
- [6] G. Angenendt, S. Zurmühlen, R. Mir-Montazeri, D. Magnor and D. U. Sauer, "Enhancing battery lifetime in PV battery home storage system using forecast based operating strategies," *Energy Procedia*, vol. 99, pp. 80-88, 2016.
- [7] D. Stroe, M. Swierczynski, A. Stroe, R. Laerke, P. C. Kjaer and R. Teodorescu, "Degradation behavior of lithium-ion batteries based on lifetime models and field measured frequency regulation mission profile," *IEEE Trans. Ind. App.*, vol. 52, no. 6, pp. 5009-5018, Nov. 2016.
- [8] D. Stroe, M. Świerczyński, A. Stan, R. Teodorescu and S. J. Andreasen, "Accelerated lifetime testing methodology for lifetime estimation of lithium-ion batteries used in augmented wind power plants," *IEEE Trans. Ind. App.*, vol. 50, no. 6, pp. 4006-4017, Nov. 2014.
- [9] D. Farinet, M. Maurer, L. Vacca, S. V. Spataru and D. Store, "Battery lifetime analysis for residential PV-battery system used to optimize the self consumption - a Danish scenario," *IEEE Energy Conversion Congress and Exposition (ECCE)*, pp. 6693-6698, Nov. 2019.
- [10] A. Marongiu, T. Pavanarit and D. U. Sauer, "Influence of current and temperature variation on a LiFePO_4 battery total capacity," *2013 World Electric Vehicle Symposium and Exhibition*, Oct. 2014.
- [11] S. Grolleau, A. Delaille and H. Gualous, "Predicting lithium-ion battery degradation for efficient design and management," *World Electric Vehicle Symposium and Exhibition (EVS27)*, Oct. 2014.
- [12] M. Huang and M. Kumar, "A case study into impacts of usage patterns on lithium-ion battery aging through incremental capacity analysis based health monitoring," *Prognostics and System Health Management Conference (PHM-Paris)*, Jul. 2019.
- [13] M. Jafari, A. Gauchia, K. Zhang and L. Gauchia, "Simulation and analysis of the effect of real-world driving styles in an EV battery performance and aging," *IEEE Trans. Transp. Electrification*, vol. 1, no. 4, pp. 391-401, Dec. 2015.
- [14] E. Sarasketa-Zabala, E. Martinez-Laserna, M. Berecibar, I. Gandiaga, L. M. Rodriguez-Martinez and I. Villarreal, "Realistic lifetime prediction approach for Li-ion batteries," *Appl. Energy*, vol. 162, pp. 839-852, Jan. 2016.
- [15] J. D. K. Bishop, C. J. Axon, D. Bonilla, M. Tran, D. Banister and D. McCulloch, "Evaluating the impact of V2G services on the degradation of batteries in PHEV and EV," *Appl. Energy*, vol. 111, pp. 206-218, Nov. 2013.
- [16] A. Marongiu, M. Roscher and D. U. Sauer, "Influence of the vehicle-to-grid strategy on the aging behavior of lithium battery electric vehicles," *Appl. Energy*, vol. 137, pp. 899-912, Jan. 2015.
- [17] S. Bai and S. M. Lukic, "Unified active filter and energy storage system for an MW electric vehicle charging station," *IEEE Trans. Power Electron.*, vol. 28, no. 12, pp. 5793-5803, Dec. 2013.
- [18] H. S. H. Chung, H. Wang, F. Blaabjerg, and M. Pechut, "Reliability of power electronic converter systems," *IET*, 2015.
- [19] A. B. Khan and W. Choi, "Optimal charge pattern for the high-performance multistage constant current charge method for the li-ion batteries," *IEEE Trans. Energy Conversion*, vol. 33, no. 3, pp. 1132-1140, Sep 2018.
- [20] U. Iraola, I. Aizpuru, J. M. Canales, A. Etxeberria and I. Gil, "Methodology for thermal modelling of lithium-ion batteries," *IECON 2013 - 39th Annual Conference of the IEEE Ind. Electron. Society*, pp. 6752-6757, Jan 2014.
- [21] H. Huang and P. A. Mawby, "A lifetime estimation technique for voltage source inverters," *IEEE Trans. Power Electron.*, vol. 28, no. 8, pp. 4113-4119, Aug 2013.

- [22] M. Ecker, J. B. Gerschler, J. Vogel, S. Käbitz, F. Hust, P. Dechent, and D. U. Sauer, "Development of a lifetime prediction model for lithium-ion batteries based on extended accelerated aging test data," *Journal of Power Sources*, pp. 215:248-257, 2012.
- [23] M. Broussely, P. Biensan, F. Bonhomme, P. Blanchard, S. Herreyre, K. Nechev, and R.J. Staniewicz, "Main aging mechanisms in li ion batteries," *Journal of Power Sources*, vol. 146, no. 1-2, pp. 90-96, 2005.
- [24] J. Wang et al., "Cycle-life model for graphite-lifepo4 cells," *Journal of Power Sources*, vol. 196, no. 8, pp. 3942-3948, 2011.
- [25] R.B Wright et al., "Power fade and capacity fade resulting from cycle-life testing of advanced technology development program lithium-ion batteries," *Journal of Power Sources*, vol. 119-121, pp. 865-869, 2003.
- [26] D. Store, "Lifetime models for Lithium Ion batteries used in virtual power plants," *Electrical Engineering Doctor of Philosophy Thesis*, 2014.
- [27] M. Safari, M. Morcrette, A. Teyssot and C. Delacourt, "Life-prediction methods for lithium-ion batteries derived from a fatigue approach I. Introduction: Capacity-loss prediction based on damage accumulation," *Journal of the Electrochemical Society*, vol. 157, pp. A713-A720, 2010.
- [28] P. D. Reigosa, H. Wang, Y. Yang, and F. Blaabjerg, "Prediction of bond wire fatigue of IGBTs in a PV inverter under a long-term operation," *IEEE Trans. Power Electron.*, vol. 31, no. 10, pp. 7171-7182, Oct 2016.
- [29] A. Sangwongwanich, Y. Yang, D. Sera, F. Blaabjerg and D. Zhou, "On the impacts of PV array sizing on the inverter reliability and lifetime," *IEEE Trans. Ind. App.*, vol. 54, pp. 3656-3667, 2018.
- [30] M. Sandelic, A. Sangwongwanich and F. Blaabjerg, "Reliability evaluation of PV systems with integrated battery energy storage systems: DC-coupled and AC-coupled configurations," *MDPI Electron.*, vol. 8, no. 9, pp. 1059-1077, Sep 2019.